Science and Engineering Research Council
Rutherford Appleton Laboratory
Chilton DIDCOT Oxon OX11 0QX

RAL-93-058

Basic Concepts for the Interpretation of Neutron Scattering Experiments at an Atomic Level of Description

S W Lovesey

July 1993

Basic Concepts for the Interpretation of Neutron Scattering Experiments at an Atomic Level of Description

Stephen W. Lovesey, Rutherford Appleton Laboratory, Oxfordshire, U.K.

Contents

Prepared for the Summer School on Neutron Scattering, Zuoz, (15-21 August, 1993)

1. Prologue

All text books on solid-state physics, and most text books on the broader scope of condensed matter physics, report experimental results obtained by the technique of neutron scattering. In fact, neutron beam techniques contribute not only to studies in these fields of research but also biology, materials science, chemistry, and various forms of industrial research (radiography, small angle scattering, resonance thermometry, etc.). One of the great attractions is that measured quantities are related quite directly to atomic-level variables used to describe basic properties of materials, such as, lattice vibrations (phonons), spin waves (magnons), excitons, and spatial distribution functions for nuclei and magnetic atoms. In view of this, it is not really surprising that data obtained with neutron beam techniques pervade so many branches of science, or that there is a tradition of strong exchanges between neutron beam experimental studies and theoretical chemistry and physics (analytic and computational studies).

The aim of these notes is to provide some information on basic *concepts* for the interpretation of neutron scattering experiments at an atomic level of description. The presentation is very much at the descriptive level, so there are no examples of the actual working out (algebra) to be done in arriving at results. Readers who wish to see such detail can consult one of the many cited review articles and books.

In compiling the references, preference has been given to recent works which are pertinent to the covered topics or which themselves give full references to earlier relevant literature. The interested reader can then refer back through the literature, if desired.

2. Neutron properties

The utility of neutron scattering as an atomic-scale probe of condensed matter stems from the relative weakness of neutron-matter scattering, the compatibility of neutron energies and wavelengths with characteristic energies and lengths of atomic motions in solid and liquids, and the magnetic moment of the neutron (Scherm, 1988). The neutron-matter interaction is so weak that first-order perturbation theory is wholly adequate to account for the slow neutron scattering cross-section (This point might need clarification since neutron-proton scattering involves what particle physicists call strong interactions - the interaction between hadrons with a coupling constant large compared to the fine structure constant $\simeq 1/137$. Nevertheless, the scattering of slow neutrons by nuclei (neutron energies ~ few eV) is adequately described by first-order perturbation theory - Born approximation - using an appropriate (Fermi) pseudo-potential which, in fact, is so simple that it is characterized by a single complex number, usually called the

scattering length). In other words, neutron scattering provides information on the chemical and physical properties of matter that is undistorted by the radiation. Furthermore, the interpretation of the measured cross-section is not clouded by uncertainty about the nature of the radiation-matter interaction or specification of the cross-section.

Neutrons interact with the nuclei and electrons in matter, and the scattering cross-sections are similar in magnitude. It is possible to discrimate between scattering events involving nuclei and electrons. In consequence, the neutron scattering technique provides unambiguous information on the positions and motions both of nuclei and of electrons. Moreover, since neutrons penetrate deeply into matter they provide an ideal probe of the bulk properties of matter. (However, neutrons are also absorbed in matter.) In the past few years there has been an expolosion of activity in the use of neutron (near critical) reflection to study surfaces and interfacial phenomena (Penfold and Thomas, 1990 and Russell, 1990).

Neutron nuclear scattering, as well as the absorption, cross sections vary from isotope to isotope in a more or less random manner. In many applications it is particularly advantageous that the scattering cross sections for the proton and deuteron are very different. The cross section for a proton is a massive 82 barns (1 barn = 10^{-24}cm^2) whereas for a deuteron it is an order of magnitude smaller. Hence, the proton function in macromolecules, membranes, etc., is readily studied, while deuteration enables us to pick out properties of the host environment. The magnitude of neutron scattering and absorption cross sections for some selected nuclei are given in Table 1.

The energy E for a neutron with a wave vector $\mathbf{k}$ is

$$E = \hbar^2 k^2 / 2m, \qquad (1)$$

where $k = |\mathbf{k}|$ and m is the neutron mass. Energies are often given in units of meV = 10^{-3}eV, and $(\hbar^2/2m) = 2.08$ meV Å^{-2}. In terms of the neutron wavelength λ we have,

$$\lambda = (h^2 / 2mE)^{1/2} = 9.04\, E^{-1/2} \qquad (2)$$

where λ is in Å and E is in meV. Here we have chosen the energy unit favoured by physicists. Other energy units frequently used in spectroscopy are related to the meV through

1 meV ≡ 0.24 THz ≡ 8.07 cm^{-1} ≡ 11.61 K,

and the conversion to temperature is included for completeness. (It is also useful to remember $\hbar \simeq 0.66$ meV ps.)

It is perhaps useful at this junction to recall that, in contrast to neutron scattering from materials, photon scattering (Agarwal, 1991) is dominated by the photon-electron interaction, described by quantum electrodynamics. Absorption of photons due to the photo-electric process and Compton effect severely reduce photon penetration in matter, and so the technique is highly surface sensitive. The photon-matter interaction contains complicated processes, some of which involve nonlinear events not described within the framework of linear response theory that underpins the interpretation of neutron scattering (excluding events that involve compound nuclear resonance states).

The high intensity of photon beams from electron synchrotron sources make it feasible to exploit magnetic photon scattering (a relativistic correction to the Thompson amplitude) as a probe of condensed matter (Lovesey, 1993a). This technique has some advantages with respect to magnetic neutron scattering, although it is likely to be confined in the near future to elastic (diffraction) and Compton scattering studies for the most part.

By and large, selection rules, which are manifestations of high symmetry conditions, operate more forcefully in photon scattering than in neutron scattering. In optical spectroscopy, for example, the change in photon wave vector, K, is so small that events are restricted by the dipole selection rule, whereas in a corresponding neutron induced event K can be relatively large and additional processes are engaged. Similar reasoning holds for the excitation of states in a crystal. Selection rules are manifest at points of high symmetry in the Brillouin zone, such as the zone centre and boundary, and generally absent at an arbitrary point on a dispersion curve.

3. A potted history

Joliot-Curie's communication of 28 January 1932, reported that alleged γ-rays from the α-beryllium reaction were capable of ejecting protons from paraffin. When the paper reached Chadwick, at the Cavendish Laboratory, he went to work and on 17 February submitted a paper entitled "possible existence of a neutron" in which he proposed that the α-beryllium reaction is $\alpha + {}^{9}\mathrm{Be} = {}^{12}\mathrm{C} + \mathrm{n}$. Chadwick's discovery of the neutron, in a few days of strenuous work, concluded a search that, off and on, had been conducted at the Cavendish for more than a decade.

In early 1934 Fermi submitted the first in a series of articles on radioactivity induced by neutron bombardment. With this paper Fermi started experimental studies in neutron physics that made him perhaps the world's leading authority on the subject during the nineteen thirties. His pseudopotential method, applied to neutron scattering by nuclei in condensed matter, appeared in 1936 and it remains the cornerstone of the interpretation of low energy neutron-nucleus scattering experiments.

In the same year Bloch predicted that the electromagnetic neutron-neutron amplitude is similar in magnitude to the classical electron radius, and therefore comparable to nuclear scattering amplitudes. The following year Schwinger queried Bloch's calculation: the latter is now known to be incorrect, and Schwinger provides the correct result although his reasoning is erroneous. A correct calculation, and physical interpretation, is provided by Migdal in a paper submitted in July 1938 to a Russian Journal. However, Migdal's work was unnoticed in the West, and the alleged Bloch-Schwinger controversy was finally settled in 1951 when two independent experiments found unambiguous evidence to support the result given by Schwinger, the basis of the interpretation of neutron-electron scattering experiments is the paper by Halpern and Johnson published in 1939. (Although these authors subscribe to the Schwinger view they nevertheless propose experiments to settle the Bloch-Schwinger controversy.)

The major sources of neutrons in the early nineteen thirties were radium-beryllium sources. Even though it was possible to demonstrate the diffractive properties of neutrons, the low intensities from radium-beryllium did not permit the practical use of neutron beams to study the properties of condensed matter. The latter began to flourish with the development of nuclear reactors. The Oak Ridge Graphite Reactor and the CP-3 reactor at the Argonne National Laboratory became operational in 1943 and 1944, respectively.

Neutron intensities produced by modern, high-flux reactors are three orders of magnitude larger that those obtained with the early reactors at the Oak Ridge and Argonne Laboratories. Moreover, new vistas have been opened with advanced spallation sources which utilize protons to liberate a very large supply of energetic neutrons from heavy metal targets (Williams and Lovesey, 1989 and Tomkinson et al., 1991). The ISIS spallation source is pulsed (50 Hz) whereas SINQ at PSI, to be commissioned in the next few years, is continuous like most reactor neutron sources.

4. Perspective

The geometry of a neutron scattering experiment is sketched in Fig. (1), which also serves to define some notation. Not mentioned in the figure are the states of polarization of the incident and scattered neutron beams. Polarization analysis offers some very significant advantages but, unfortunately, the accompanying intensity penalty is often too large (Williams, 1988). Even so, various spectrometers exist at reactor sources and their use, particularly for studies of magnetic materials, have produced very interesting scientific results (Böni, 1993) that are possibly not obtainable by other experimental techniques.

In a neutron scattering experiment one measures the fraction of neutrons of incident energy E scattered into an element of solid angle $d\Omega$ with an energy between E′ and (E′ + dE′). The measured quantity is the partial differential cross-section, denoted by

$$(d^2\sigma / d\Omega dE')\cdot$$

The cross-section σ has the dimension of area, and so the partial differential cross-section has the dimension of (area/energy.solid angle).

In more general terms, the quantity $(d^2\sigma/d\Omega dE')$ is a measured response function; it provides the response of the target sample to an incident beam with energy E and wave vector **k** (and possibly a finite polarization). As such, it is a purely real quantity which is positive or possibly zero. Since slow neutron scattering is a weak process, the formalism for interpretation of data on $(d^2\sigma/d\Omega dE')$ is linear response theory; this is based on Fermi's Golden Rule for transition rates or, equivalently, the first Born approximation in scattering theory (Lovesey, 1986). With regard to the latter, it is perhaps worth mentioning that the theory we describe comes under the heading of the kinematical theory of neutron scattering that neglects macroscopic multiple-scattering effects. In the case of Bragg reflection from crystals, these multiple-scattering effects are referred to as dynamical diffraction effects and include, for example, extinction and anomalous absorption. Dynamical and kinematical theories of diffraction are associated with the names of Ewald and Laue, respectively. (The distinction between dynamical and kinematical theories of diffraction is meaningful only for radiation for which the index of refraction is close to unity; cf. Sears 1989).

Once can contrast neutron scattering, and NMR and muon spin resonance, by the observation that resonance experiments provide information on bulk response functions whereas neutron scattering measures a differential response function, i.e. the relaxation times T_1 and T_2 are akin to the specific heat, say (integrals over relevant degrees of

freedom). Hence, a neutron scattering experiment is seen to provide a wealth of detailed information on the static and dynamic properties of the sample.

Linear response theory, which underpins most experiments that probe properties of condensed matter (including neutron scattering but excluding, for example, photoemmission) is often written in terms of correlation functions depend on time (t) and spatial co-ordinates (**R**) and usually written $\langle A(\mathbf{R},t)\ B\ (\mathbf{R}',t')\rangle$ where A and B are quantum mechanical operators for observable quantities (in which case A, B are Hermitian operators) and the angular brackets denote a thermal average. Such a correlation function is a complex quantity, and for A = B the imaginary component is related to quantum aspects of the system. The neutron cross-section is proportional to the Fourier transform of $\langle A(\mathbf{R},t)\ A\ (\mathbf{R}',t')\rangle$ with respect to time and spatial co-ordinates; the conjugate variables in the Fourier transforms are the energy ($\hbar\omega$) and wave vector (**K**) transfers, respectively.

5. Some examples of cross-sections

Since the scattering of slow neutrons is a weak process it can be described by first-order perturbation theory, i.e., Fermi's Golden Rule for transition rates. In consequence, we treat the incident and scattered neutron states as plane waves with energies E,E' and wave vectors $\boldsymbol{k},\boldsymbol{k}'$, related as in eq. 1, and illustrated in Fig. (1). The cross-section, or response function, is described in a four dimensional space spanned by the variables

$$\hbar\omega = E - E' \tag{3}$$

and

$$\mathbf{K} = k - k' \tag{4}$$

If the target sample is spatially isotropic the response function depends only on ω and $K = |\mathbf{K}|$.

The differential cross-section is readily expressed in terms of correlation functions that are determined solely by the chemical and physical properties of the target sample. This is by far the most elegant and powerful representation, and the one adopted here. Further details, including an exposition of linear response theory, are found in Lovesey (1986) and Lovesey (1987). We will separately describe nuclear and magnetic scattering, though some basic concepts are common to both, of course. A wide ranging

review of neutron scattering science is found in the many articles gathered in a three-volume treatise edited by Price and Sköld (1986).

5.1 Nuclear scattering

Slow neutron scattering is described by a single parameter, namely a scattering length b which is assumed to have minimal energy dependence. The imaginary part of b gives rise to absorption. This is extremely large for some isotopes, e.g., about 15000 barns for He^3 and 5Å neutrons.

The nuclear scattering cross-section is a scattered length weighted sum of correlation functions. Let i,j label the scattering nuclei, and denote the correlation function by $Y_{ij}(\mathbf{K},t)$. With this notation the partial differential cross-section is,

$$\frac{d^2\sigma}{d\Omega dE'} = (E/E')^{1/2} \int_{-\infty}^{\infty} dt (1/2\pi\hbar) e^{-i\omega t} \sum_{ij} b_i^* b_j Y_{ij}(K,t), \qquad (5)$$

where $d\Omega$ is the solid angle subtended by the detector as shown in Fig. (1). The function $Y_{ij}(\mathbf{K},t)$ possesses properties that make the right-hand side of (5) both real and either positive or zero, as required for a response function. It is necessary to average the cross-section over the distribution of nuclear spins (assumed to be completely random), isotopes, substitutional disorder, etc. We will deal with those averages as and when required.

5.1.1 *Purely elastic scattering.* This is generated by the value of the correlation function at infinite time; $Y_{ij}(\mathbf{K}, \infty)$ with $\mathbf{K} \neq 0$ is finite for crystals and fully arrested supercooled liquids, for example, but vanishes for normal liquids. For a crystal, it is customary to write,

$$Y_{ij}(\mathbf{K},\infty) = \exp\{i\mathbf{K}\cdot(\mathbf{R}_i - \mathbf{R}_j) - W_i(\mathbf{K}) - W_j(\mathbf{K})\} \qquad (6)$$

where $\mathbf{R}_i$ is the equilibrium lattice position of the i'th atom and the remaining terms are Debye-Waller factors. An explicit expression for W(K) valid for a harmonic lattice is given following eq. (16).

Bragg scattering is elastic and coherent and occurs under special geometrical conditions. It is generated by a perfect crystal, which means that the appropriate cross-section is formed with the square of the average of the effective scattering length per unit cell. Let the crystal contain N unit cells of volume υ_0 in which the atoms are at sites defined by position vectors $\mathbf{d}$. The elastic coherent cross-section is then

$$\left(\frac{d\sigma}{d\Omega}\right)^{el}_{coh} = N((2\pi)^3/v_o)\sum_{\tau} |F_N(\tau)|^2 \delta(K-\tau) \quad (7)$$

in which $\{\tau\}$ are reciprocal lattice vectors and the unit cell structure factor,

$$F_N(K) = \sum_d \bar{b}_d \exp(iK\cdot d - W_d(K)) \quad (8)$$

where b is the scattering length averaged over isotope and nuclear spin distributions; representative examples of b are provided in Table I. From (7) it is evident that scattering occurs only when the condition $\tau = K$ is satisfied, which is a statement of Bragg's Law.

The difference between the total elastic scattering and the Bragg intensity from a solid is due to disorder and defects in the crystal, nuclear spins and mixtures of isotopes. By definition, it is not coherent and it occurs to some extent at all scattering angles. It is customary, but not completely logical, to use the term incoherent scattering for non-Bragg scattering generated by nuclear spins and isotope mixtures (note that a sample of a pure isotope can produce incoherent scattering if the nuclear spin is finite, e.g., He^3). All the remaining non-Bragg scattering is called diffuse scattering.

Incoherent elastic scattering from a crystal measures the quantity,

$$N\sum_d [\overline{b_d^2} - (\bar{b}_d)^2] \exp[-2W_d(K)] \quad (9)$$

This can be interpreted as the sum over atoms in the unit cell of the Debye-Waller factor weighted by the mean-square fluctuation in the scattering length.

As an example of elastic diffuse scattering consider a binary system in which type-2 atoms (impurity atoms, say) occur with concentration *c*. All other things being equal apart from a difference in coherent scattering lengths, diffuse scattering occurs which is proportional to,

$$(\bar{b}_2 - \bar{b}_1)^2 c(1-c). \quad (10)$$

A more realistic model would allow for the difference in Debye-Waller factors and the deformation in the host lattice created by the impurity atoms. In the latter case, the appropriate cross-section is proportional to the absolute square of the spatial Fourier transform of the deformation, which can be compared to theoretical predictions. For

more information on the use of neutron scattering to study material properties such as defects see, for example, the volumes edited by Kostorz (1979) and Price and Sköld (1986).

5.1.2 *Total scattering.* For a liquid strictly elastic events occur only if K = 0, which corresponds to no scattering. Hence, the total scattering is measured in a neutron scattering experiment without energy analysis. This quantity is the response function integrated over all neutron energy transfers. With a monatomic sample, in which quantum effects are negligible (achieved with large A atoms at relatively high temperatures), the total coherent scattering, at constant K, is proportional to the structure factor,

$$S(K) = 1 + \rho_0 \int dr\, e^{iKr}[g(r) - 1], \tag{11}$$

in which ρ_0 is the particle density and g(r) is the pair distribution function. It is perhaps, useful to note that $r^2g(r)$ is the probability distribution for the particle density about the origin. Hence, the number of particles within a sphere of radius R prescribed about a given particle is

$$4\pi\rho_0 \int_0^R dr\, r^2 g(r) \quad . \tag{12}$$

In the limit $R \rightarrow \infty$ this quantity approaches the total number of atoms in the sample, as required.

Before turning to inelastic scattering we draw attention to a basic difference between Bragg scattering and total scattering. The latter is readily shown to be proportional to $Y_{ij}(K,0)$, i.e., the instantaneous value of the correlation function. On the other hand, Bragg scattering is proportional to the square of a time-averaged variable (a basic principle in statistical physics is that statistical averaging is completely equivalent to time averaging). The difference between these two extreme limits of the correlation function is related to the appropriate isothermal susceptibility, i.e., the mean-square fluctuation in the number density. We conclude that the difference is small except in the vicinity of a phase transition, when fluctuations take macroscopic values. One final point to make is that total scattering is often referred to as the static approximation to the cross-section, the choice of terminology being more or less self-evident in view of what we have just said.

5.1.3. *Spectroscopy.* This corresponds to scattering events for which $\omega \neq 0$ and thus are termed inelastic. It is customary to use the label quasi-elastic for the part of the

inelastic spectrum which arises from random, or stochastic, processes that occur over relatively long time scale (Bee, 1989), e.g., diffusive motion of an atom in a liquid. If classical statistics apply, the incoherent (single-particle) scattering cross-section is in this case determined by the correlation function

$$Y(K,t) \sim \exp(-K^2 D|t|) \tag{13}$$

where D is the self-diffusion constant. The corresponding cross-section is,

$$\frac{d^2\sigma}{d\Omega dE'} = \left(\frac{E}{E'}\right)^{1/2} \frac{\sigma_i}{4\pi^2} \frac{K^2 D}{\omega^2 + (K^2 D)^2} \tag{14}$$

in which σ_i is the incoherent cross-section (79.8 barns and 2.0 barns for a proton and deuteron, respectively). A similar result holds for a particle jumping between interstitial sites of a lattice, e.g., hydrogen diffusion in metals. In this instance $D = l^2/\tau$, where l is a length, of order the lattice constant, and τ is the residence time at a given site.

The generic form of the correlation function that appears in quasi-elastic scattering is, to a good approximation,

$$Y(K,t) = \exp(-K^2 \mu(t)/2), \tag{15}$$

in which $3\mu(t)$ is the mean-square displacement after a time t. The result $\mu(t) \sim |t|$ found for uncorrelated jumps on a lattice is characteristic of a random-walk process.

If a particle is bound in a crystal, or macromolecule, then often a useful starting point is to consider scattering from a harmonically bound particle. The scattering response for a particle with a natural frequency ω_0 is,

$$\exp[-2W(K)+(1/2)\hbar\omega\beta] \sum_{n=-\infty}^{\infty} I_n(y)\, \delta[\hbar\omega - n\hbar\omega_0]\,. \tag{16}$$

The interpretation of (16) is straightforward; the scattering vanishes unless $\omega = n\omega_0$, and the integer n measures the number of units of energy $\hbar\omega_0$ lost ($n > 0$) or gained ($n < 0$) by the neutron. The various quantities in (16) are; $\beta = 1/k_B T$ (T is the absolute temperature), $I_n(y)$ is a Bessel function of the first kind, and using the dimensionless variables $x = (\hbar\omega_0\beta/2)$ and $\gamma = (\hbar K^2/2M\omega_0)$ where M is the mass of the scattering particle, $y = \gamma/\sinh(x)$ and $W = (\gamma/2)\coth(x)$. Note that the elastic contribution ($n = 0$) contains $I_0(y)$. This factor arises from thermal fluctuations of the bound particles, which are negligible if the particle participates in a bulk collective motion.

The terms in (16) with n = ±1 are usually labelled the fundamental modes. If y « 1, as is often the case, the intensity of high-order modes is very small in comparison with the fundamental since,

$$I_n(y) \sim (1/n!)y^{|n|}; y \to 0.$$

In the limit $(\hbar K^2/M\omega_0) \gg 1$, which can be achieved with a pulsed neutron source, it is not possible to select the fundamental mode in the response. A palisade of modes of near equal amplitude are engaged in scattering, so the expansion leading to the representation (16) is of minimal value. It can be shown that, in the limit of large K, the scattering response tends to a Gaussian envelope function centred at the recoil energy $(\hbar K)^2/2M$ with a mean-square width of $2\omega_0^2 W(K)$.

A far more realistic model of single particle dynamics is achieved by considering the particle as a defect in a host matrix. Two parameters characterize the particle-matrix system, namely the ratio of the two masses and the deviation of the particle-matrix stretching force from that in the bulk matrix. The dynamics of the particle can be obtained in closed form if the stretching forces are harmonic. Calculations with this model reveal that a light mass (e.g. proton in a macromolecule) creates a high frequency mode which is well separated from the maximum phonon frequency in the pure host. By using a Debye model for the latter the frequency of the new mode is

$$\omega = (0.6M/M')^{1/2}\omega_D,$$

where (M/M′) is the host-particle mass ratio, assumed to be large, and ω_D is the Debye frequency. This formula accounts for hydrogen mode frequencies in metal-hydrogen systems apart from those using palladium, which display other slightly unusual properties (Kostorz, 1979).

Detailed numerical calculations of the scattering response for a particle embedded in a matrix show that it contains a myriad of features. For the two extreme cases of $K \to 0$ and $K \to \infty$ the response is well approximated by the fundamental contributions and a Gaussian envelope function, respectively. But, for intermediate K the line shapes are highly structured. Satellites to the harmonics appear which can be traced back to structure in the host density of states. Such features are understood by viewing the light mass particle as a probe of host lattice vibrations.

We return now to scattering from collective atomic motions, or phonons. Neutron scattering is the established method of measuring phonon dispersion curves. To understand how this is possible consider the fundamental contribution to the harmonic

oscillator response given in eq. (16); this vanishes unless the neutron energy change matches the energy of one quantum. When scattering from a collective motion the energy selection-rule is supplemented by a wave vector selection-rule, $\mathbf{K} = \mathbf{q} + \boldsymbol{\tau}$ wher $\mathbf{q}$ is the lattice wave vector (confined to a Brillouin zone) which labels the phonon mode. In an experiment both K and ω are determined, and hence a point on the phonon dispersion curve is established.

The one-phonon scheme we have just described has no value in tackling the interpretation of coherent scattering from a liquid for which two extreme limits are well understood. For small K and ω we can appeal to linear hydrodynamics. The response for fixed K is found to consist of an elastic peak (Rayleigh line) and two inelastic peaks (Brillouin lines) at $\omega = \pm Kc_0$ where c_0 is the velocity of sound. In the opposite limit of large K the response resembles that of a free particle, namely a Gaussian centred at the recoil energy $E_R = (\hbar K)^2/2M$ with a mean-square width proportional to $(k_B T E_R)$. While much has been learnt about the nature of physical processes engaged at intermediate K, the subject is on-going, particularly with regard to molecular liquids and the super-cooled state.

5.2. Magnetic scattering

Neutrons scatter off the magnetic field generated by unpaired electrons in a sample. Note that the number of electrons involved is generally a small fraction of those engaged in an X-ray experiment. In the latter case, charge (Thomson) scattering engages all electrons whereas in magnetic, neutron or photon, scattering it is only the relatively small fraction of unpaired electrons that contribute to the scattering process.

The magnetic field has two sources. First, the spins of electrons lead to a dipole-dipole interaction. Second, mobile electrons generate a field obtained from Biot-Savart's formula. In the forward direction ($K \rightarrow 0$) the neutron-electron interaction is simply related to the total magnetic moment. Here, for an atom characterized by total spin and angular momentum **S** and **L**, respectively, the forward scattering amplitude is generated by $(\mathbf{L} + 2\mathbf{S})$.

The general form of the neutron-electron interaction for arbitrary K is quite complicated. Calculation of the matrix elements required in the interpretation of neutron-electron spectroscopy of isolated ions requires the full battery of Racah algebra used in atomic and nuclear spectroscopy (Balcar and Lovesey, 1989). Even so, we can give insight into the behaviour of magnetic neutron scattering by employing a relatively simple expression for the interaction, valid for modest values of K.

5.2.1. *Purely elastic scattering.* For not too large K, the magnetic interaction operator is

$$r_0\,(1/2)gF(K)\mathbf{J} \tag{17}$$

where the interaction strength r_0 = - 0.54 x 10^{-12}cm, g $\boldsymbol{J}$ is the magnetic moment operator and F(K) is an atomic form factor. For a spin-only ion g$\boldsymbol{J}$ $\rightarrow 2\boldsymbol{S}$, whereas for a rare earth ion $\boldsymbol{J} = \boldsymbol{L} + \boldsymbol{S}$ and g is the Lande splitting factor. The form factor is defined to be unity in the forward direction, and decreases monotonically to a value of ~ 0.2 at K ~ 8Å^{-1} in a typical case.

The definitions of Bragg and total scattering carry over from the previous discussion of nuclear scattering. We begin our discussion with the total scattering from N paramagnetic ions, namely,

$$\frac{d\sigma}{d\Omega} = N[(r_0/2)gF(K)]^2(2/3)J(J+1), \tag{18}$$

where J is the magnitude of the spin, i.e. $\boldsymbol{J}\cdot\boldsymbol{J} = J(J+1)$. This formula shows that the cross-section is large for large values of J, just as we might expect from physical intuition. The dependence on the scattering vector K comes only through the form factor F(K).

There is, of course, a very strong K dependence in Bragg scattering from an ordered magnetic material. First, scattering vanishes unless $\mathbf{K} = \boldsymbol{\tau}$ where $\{\boldsymbol{\tau}\}$ are reciprocal lattice vectors for the magnetic structure. A second dependence arises from the fact that the componenet of $\boldsymbol{J}$ perpendicular to K is observed. This feature often enables the moment orientation to be established. No such factor is explicit in (18) because the paramagnetic ions are randomly orientated. The Bragg cross-section for a collinear magnetic structure is,

$$\left(\frac{d\sigma}{d\Omega}\right)^{el}_{coh} = r_0^2N((2\pi)^3/v_0)\sum_{\boldsymbol{\tau}}\delta(\mathbf{K}-\boldsymbol{\tau})e^{-2W(\tau)}|F_M(\boldsymbol{\tau})|^2[1-(\hat{\boldsymbol{\tau}}\cdot\hat{\boldsymbol{\eta}})^2], \tag{19}$$

where $\hat{\boldsymbol{\eta}}$ is a unit vector that defines the preferred magnetic (easy) axis and

$$F_M(K) = \sum_d (1/2)g_d <J> F_d(K)\xi_d e^{i\mathbf{K}.\mathbf{d}}, \tag{20}$$

in which $\xi_d = \pm 1$ according to the orientation of the magnetic moment relative to the referred axis. Several features merit explicit mention. The total Bragg scattering from a magnetic material is described by the sum of (7) and (19). The moment, proportional to the thermal average <J>, vanishes at the phase transition to the paramagnetic state.

Bragg intensities can be used to obtain the critical exponent for the continuous decrease of the magnetization in the immediate vicinity of the transition. A magnetic material usually forms domains, in which case the orientation factor $\{1-(\hat{\tau}\cdot\hat{\eta})^2\}$ must be averaged over the easy axes for $\hat{\eta}$. If all directions in space were equally likely, then clearly $(\hat{\tau}\cdot\hat{\eta})^2$ would average to (1/3). The same result is also correct for cubic symmetry.

Diffuse magnetic scattering is observed with a mixed system. If one component of a binary system occurs with a small concentration then the diffuse cross-section can be shown to be proportional to the square of the spatial Fourier transform of the magnetization defect created in the host matrix. Analysis of measurements on such systems has been central to the development of the theory of the electronic structure of magnetic alloys. As the temperature of the alloy is raised toward the critical temperature, the spatial range of the defect increases. In consequence, the diffuse cross-section as a function of K becomes increasingly narrow, and it is believed to be singular at the critical temperature.

5.2.2. *Inelastic events* Next we discuss the elements of neutron-electron spectroscopy. To be concrete consider the matrix elements for transitions between J-multiplets in the energy level diagram of a rare earth ion. The ion can be regarded as isolated, to a good approximation, and not subject to a significant molecular field, for example. (The expression (17) is no longer valid since it is based on the relation $\boldsymbol{L} + 2\boldsymbol{S} = \mathrm{g}\,\boldsymbol{J}$ which is retricted to a J-multiplet.)

The matrix element $\langle JM|\boldsymbol{L} + 2\boldsymbol{S}|J'\ M'\rangle$ vanishes except for $|J - J'| = 1$; thus, for small K, we observe dipole-allowed transitions. Beyond the limit of small K higher-order transitions contribute to the cross-section. Even though the higher-order transitions are very weak compared to dipole-allowed contributions they have been unambiguously observed (Osborn et al., 1991). It is found that the energy separation between multiplets is essentially the same in concentrated and dilute magnetic systems if the levels come from a single Coulomb term. Significant differences are seen in data for the two types of system for levels that belong to different terms. This feature is attributed to screening of the Coulomb interaction by conduction electrons.

Data on dilute magnetic systems are readily obtained by optical spectroscopy. This technique is constrained by the dipole-selection rule, and it is not useful for concentrated metallic magnets. At present, neutron-electron spectroscopy, which is free of both constraints, has been successfully applied to transitions with energy separations up to 2.0 eV, and the technique is very much in its infancy.

Another form of magnetic spectroscopy is the study of crystal field levels. This is now very well established as a tool for direct observation of the crystal field energy level scheme, in 3d, rare earth and actinide compounds (Furrer, 1977 and Frick and Loewenhaupt, 1986).

The introduction of exchange interactions between ions couples the single-ion crystal field states discussed in the preceding paragraph. Collective excitations are formed from phase-related linear combinations of the single-ion transitions. These exciton states, as they are usually called, display significant dispersion which can be followed throughout the Brillouin zone in many cases. The limiting factor is neutron energy, but this has been ameliorated with the development of advanced pulsed sources and appropriate time-of-flight instrumentation.

A spin wave is the coherent propagation of a single unit of spin deviation. It is, in some respects, the magnetic analogue of a phonon, in as much that the neutron cross-section vanishes unless there is simultaneous conservation of energy and wave vector. spin wave and phonon excitations can usually be distinguished in the scattered spectrum by one of several simple tests. First, spin wave intensities decrease with increasing K because of the atomic form factor, whereas phonon intensities increase, with a K^2 dependence. Secondly, a spin wave is an excitation away from an ordered state so it vanishes above the critical temperature. Hence, spin wave excitations are usually more sensitive than phonons to variations in temperature. On approaching the transition temperature spin waves soften and become more heavily damped.

Neutron polarization analysis affords a completely unambiguous method by which to identify spin waves (Lovesey, 1987 and Williams, 1988) because creation or annihilation of a spin wave induces polarization in an unpolarized neutron beam. Phonons do not produce such an effect, as might be expected from physical intuition.

Polarization analysis is even more useful when it comes to isolating paramagnetic spin fluctuation scattering, particularly when it is a case of studying a material with high transition temperature and hence a strong phonon background. In the case of a paramagnet, which does not possess a preferred axis, there is no creation of polarization. An initially polarized beam has a final polarization in the direction of K, and a magnitude controlled by the projection of the incident polarization onto K. Hence, the final polarization vanishes if the incident polarization and K are perpendicular, and it achieves a maximum value when they are parallel.

The main problem in practice has been to obtain efficient methods of producing polarized beams or of analysing the polarization of a beam scattered by the sample.

Inelastic scattering events are typically 10^{-3} of the elastic intensity, so a relatively inefficient polarizing method that is tolerable for elastic studies may render inelastic measurements impossible.

At the time of writing there is renewed interest in the dynamics of critical and paramagnetic spin fluctuations. Various experimental groups have reported, over the past few years, careful measurements of the paramagnetic response of insulating (EuO, EuS) and metallic (Fe, Ni, Pd_2 MnSn) systems. The consensus opinion is that the response evolves with increasing K from a Lorentzian-like function centred at $\omega = 0$ to a squarer or top-hat function. Recent data for Gd shows a peak at finite ω for large K, near the zone boundary, with a strong dispersion. This feature persists deep into the paramagnetic region, and it is quantitatively explained by a calculation based on the couple-mode approximation for spin fluctuations (Westhead et al., 1991).

Another feature of magnetic systems that has recently been a focus of attention is the influence of dipolar forces on paramagnetic and critical fluctuations (Böni, 1993). Dipolar forces, present to some extent in all magnetic materials, are responsible for the bulk effect of demagnetization fields. It was not until the comparatively recent development of high resolution neutron spectrometers, with polarization analysis, that their influcence on dynamic processes in the vicinity of the critical temperature became apparent, through a series of careful experiments on metallic magnets and magnetic salts. The essential features of the data are in accord with predictions obtained for a Heisenberg magnet, including dipolar interactions, treated within the coupled-mode approximation. (Lovesey, 1993b).

References

Agarwal, B.K. (1991) X-ray Spectroscopy 2nd. edition (Springer-Verlag, Berlin)

Balcar, E., and Lovesey, S.W. (1989) Theory of Magnetic Neutron and Photon Scattering (Oxford University Press)

Bee, M. (1989) Quasi-Elastic Neutron Scattering (Adam Hilger, Bristol)

Böni, P. (1993) Physica B

Frick, B., and Loewenhaupt, M. (1986) Z. Phys. B **63**, 213

Furrer, A. (1977) editor, Crystal Field Effects in Metals and Alloys (Plenum Press, N.Y.)

Kostorz, G. (1979) Treatise on Materials Science and Technology, Vol. 15 (Academic Press, N.Y.)

Lovesey, S.W. (1986) Condensed Matter Physics: Dynamic Correlations, 2nd. edition, Frontiers in Physics Vol. 61, edt. D. Pines (Benjamin/Cummings Publishing Co., California)

- (1987) Theory of Neutron Scattering from Condensed Matter, Vols. 1 and 2, 3rd editions (Oxford University Press)
- (1993a) Photon Scattering by Magnetic Solids, Rept. Prog. Phys. **56**, 257
- (1993b) J. Phys.: Condens. Matter **5**, L251

Osborn, R., Lovesey, S.W., Taylor, A.D., and Balcar, E. (1991) Handbook on the Physics and Chemistry of Rare Earths, Vol. 14 (Elsevier Science Publishing, Amsterdam)

Penfold, J., and Thomas, R.K. (1990) J. Phys.: Condens. Matter **2**, 1369

Price, D. L., and Sköld, K. (1986) Neutron Scattering: Methods of Experimental Physics, Vols 23A/B/C (Academic Press, N.Y.)

Russell, T. P. (1990) Materials Science Repts. **5**, 171

Sears, V.F. (1989) Neutron Optics (Oxford University Press)

Scherm, R. (1988), in The Art of Measurement edt. B. Kramer (VCH, Weinheim)

Tomkinson, J., Carlile, C.J., Lovesey, S.W., Osborn, R., and Taylor, A.D. (1991) Spectroscopy of Advanced Materials, Vol. 19 (John Wiley & Sons, Chichester)

Westhead, D.R., Cuccoli, A., Lovesey, S.W., and Tognetti, V. (1991) J. Phys.: Condens. Matter **3**, 5235

Williams, W.G. (1988) Polarized Neutrons (Oxford University Press)

- Lovesey, S.W. (1989) Contemporary Phys. **30**, 35

Table 1. Neutron scattering and adsorption data for some selected elements

Element	A	% abundance	$\bar{b}$	σ_s	σ_a
H	1	100.	−0.3741	81.87	0.3326
	2	0.0149	0.6674	7.63	0.000519
	3		0.494	3.03	< 0.000006
He	*		0.326	1.21	< 0.001
	3	0.00014	0.574	5.6	5333.
	4	100.	0.326	1.21	~0
Li	*		−0.203	1.40	70.5
	6	7.5	0.187	0.98	940.
			−0.026i		
	7	92.5	−0.220	1.44	0.0454
C	*		0.6648	5.564	0.00350
	12	98.89	0.6653	5.564	0.00353
	13	1.11	0.62	5.5	0.00137
	14				$< 10^{-6}$
O	*		0.5805	4.234	0.00019
	16	99.762	0.5805	4.234	0.00019
	17	0.038	0.578	4.20	0.24
	18	0.200	0.584	4.3	0.00016
Na	23	100.	0.363	3.23	0.530
Cl	*		0.9579	16.63	33.5
	35	75.77	1.17	21.62	44.1
	37	24.23	0.308	1.2	0.433
K	*		0.367	2.10	2.1
	39	93.258	0.379	2.19	2.1
	40	0.012			34.
	41	6.73	0.258	0.83	1.46
V	*		−0.0382	4.953	5.08
	50	0.25			60.
	51	99.75	−0.0414	4.946	4.9
Fe	*		0.954	11.66	2.56
	54	5.8	0.42	2.2	2.3
	56	91.72	1.01	12.8	2.6
	57	2.2	0.23	< 1.	2.5
	58	0.28	1.5	28.	1.28
Ni	*		1.03	17.56	4.5
	58	68.27	1.44	25.87	4.6
	60	26.10	0.28	0.96	2.9
	61	1.13	0.76	7.23	2.5
	62	3.59	−0.87	9.6	14.5
	64	0.91	−0.038	0.02	1.52
Ag	*		0.597	5.09	63.3
	107	51.83	0.764		38.
	109	48.17	0.419		91.
Pb	*		0.9401	11.11	0.17
	204	1.4			0.66
	206	24.1			0.0305
	207	22.1			0.709
	208	52.4			0.00049
Bi	209	100.	0.8533	9.156	0.033

$\bar{b}(10^{-12}cm)$: Coherent scattering length for bound atoms. Complex values correspond to a neutron wave length of 1 Å .

σ_s(barns): Total scattering cross section of bound atoms for thermal neutrons.

σ_a(barns: Absorption cross sections for thermal neutrons ($2200ms^{-1}$).

* Natural isotope mixture

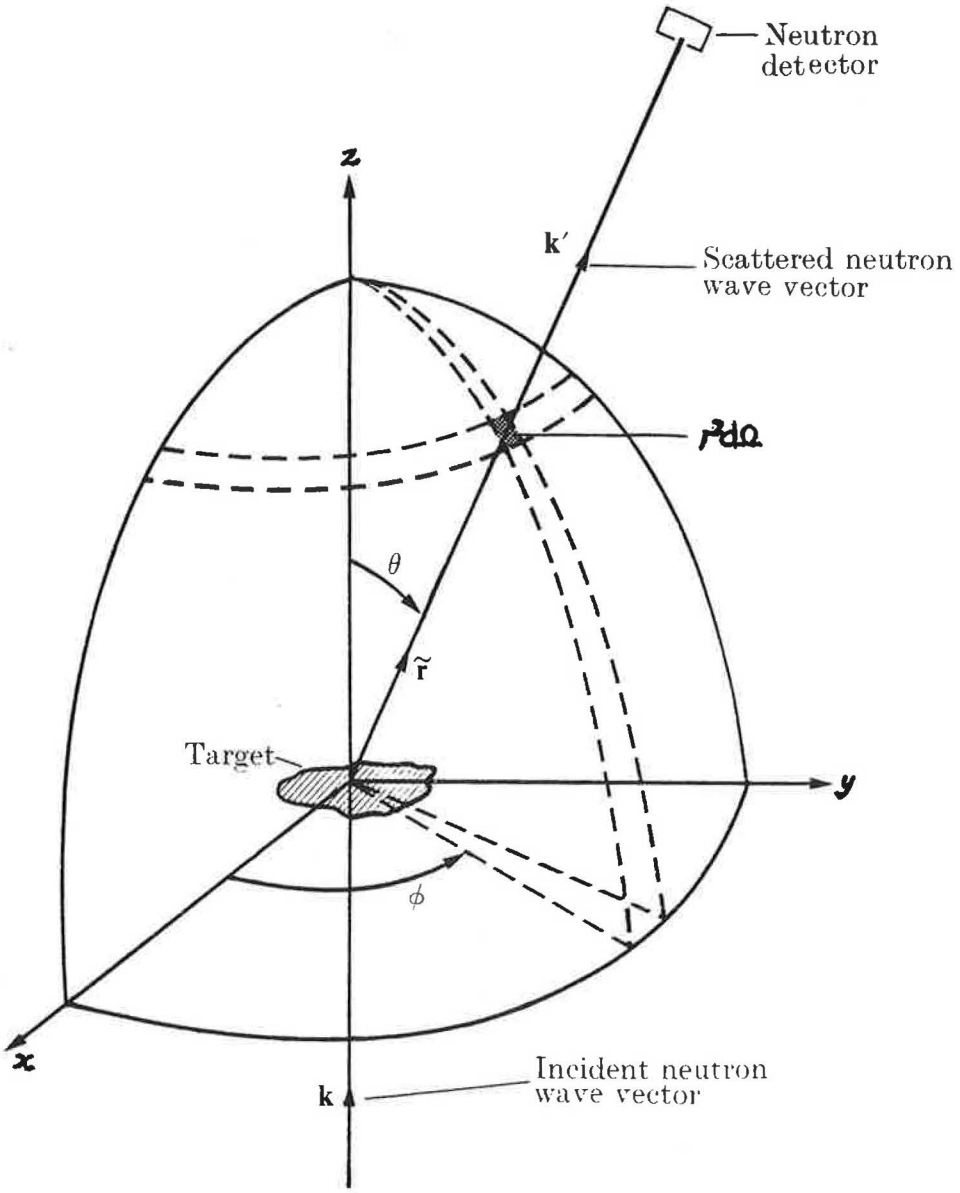

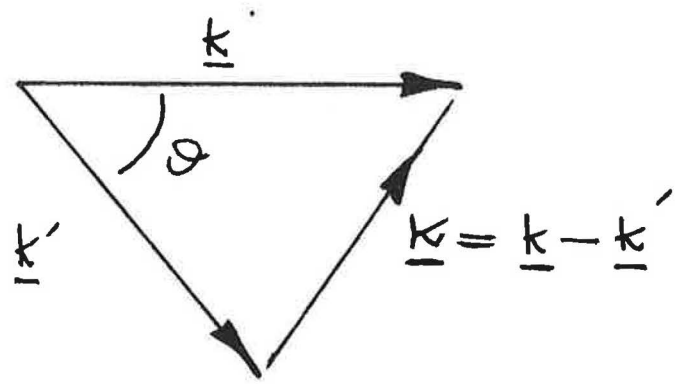

Scattering wave vector,

$$\underline{\kappa} = \underline{k} - \underline{k}'.$$

Fig. (1)